A study of Pt–Pd/γ-Al$_2$O$_3$ catalysts for methane oxidation resistant to deactivation by sulfur poisoning

Grisel Corro [a,*], Carlos Cano [a], J.L.G. Fierro [b]

[a] Laboratorio de Catálisis Ambiental, Instituto de Ciencias, Benemérita Universidad, Autónoma de Puebla. 4 Sur 104, Puebla 72000, Mexico
[b] Instituto de Catálisis y Petroleoquímica, CSIC, Cantoblanco, 28049 Madrid, Spain

A B S T R A C T

The catalytic oxidation of methane was studied over calcined and reduced Pt–Pd/γ-Al$_2$O$_3$ catalysts, in the presence and the absence of SO$_2$ in the CH$_4$–O$_2$ reaction feed. The effect of sulfation (SO$_2$ + O$_2$ for 4 h at 500 °C) was also studied on the catalyst resistance to deactivation by sulfur poisoning. Sulfating the calcined Pt–Pd/γ-Al$_2$O$_3$ catalysts resulted in a strong deactivation for the CH$_4$–O$_2$ reaction. However, the catalytic activity of the reduced-sulfated Pt–Pd/γ-Al$_2$O$_3$ catalyst for CH$_4$–O$_2$ reaction remained rather unaffected in the presence and in the absence of SO$_2$ in the reaction feed. XPS analysis revealed, over reduced-sulfated Pt–Pd/γ-Al$_2$O$_3$ catalysts, the presence of Pt(0) metallic surface species on which SO$_2$ interactions may be faster related to Pd surface species. The presence of Pt(0) may be necessary to prevent the interactions between SO$_2$ and Pd surface species. Long time catalytic tests showed that the activity of a reduced Pt–Pd/γ-Al$_2$O$_3$ catalysts for CH$_4$–O$_2$ reactions remained rather unaffected despite the presence of SO$_2$ in the reaction feed.

1. Introduction

Catalytic oxidation of methane under oxygen-rich conditions has received considerable attention. One of the reasons is the increasing interest in lean-burn natural gas vehicles (NGVs). Compared with diesel engines, NGV engines produce less NO$_x$ and particulates [1–3]. However, a problem with NGV engines is the high level of unburned methane in the exhaust. Because methane is a potent greenhouse gas, it is important to reduce the amount emitted into the atmosphere. One approach to abating methane emission is the use of catalytic exhaust converters, in which the abatement is achieved by catalytic oxidation.

Another application for catalytic oxidation of methane is in catalytic gas turbine combustors [4,5]. Instead of combusting the fuel homogeneously using a flame, the fuel is combusted over the catalysts. In this way, the combustion temperature is considerably reduced, and the formation of thermal NO$_x$ is decreased. Natural gas is a frequently used fuel in gas turbines, and the major combustible component in natural gas is methane.

A catalyst that often has been used for these applications is palladium supported on various washcoats [6]. Many studies have shown that the activity over fresh palladium-supported catalysts have poor stability for methane conversion when the temperature is kept constant [7–11]. The initial high activity when the catalysts are fresh, drops significantly during operation, resulting in increasing difficulty in igniting the methane at desirable temperatures. High concentrations of water vapor strongly inhibit the activity and also cause irreversible deactivation [6,12]. Moreover, sulfur containing compounds induce a strong deactivation by formation of stable inactive Pd sulfates [1,3]. However, Arosio et al. [13] report a regeneration strategy based on periodical natural gas pulses fed to the catalyst limiting the effects of S-poisoning of palladium catalysts. Venezia et al. [14] report a high SO$_2$ tolerant Pd supported on TiO$_2$–SiO$_2$ which presented a high methane oxidation activity.

Different additives have been used to improve the palladium catalyst. One of the more promising additives is Pt, which considerably improves the stability during reaction [7,8,15]. A considerable number of papers have also shown that the activity of the Pd–Pt catalysts is improved in comparison to the monometallic palladium catalyst [7,16–18]: no deactivation under wet conditions and improved catalytic activity possibly attributed to Pt–Pd interactions. The improved catalytic activity might not be maintained after long term use of the catalyst due to metals segregation. The resistance of Pd–Pt bimetallic catalysts against poisoning by sulfur containing compounds has not been reported yet.

Many studies of bimetallic catalysts for methane oxidation have been made using alumina as support material, and in most studies, catalysts were prepared by impregnation of the alumina with solutions of palladium and platinum nitrate. The catalysts were in all cases dried and only calcined at different temperatures [7–9,15,16,19,20], but no reducing step in hydrogen at high temperature was performed to obtain the final catalyst.

* Corresponding author. Fax: +52 222 2295551.
E-mail address: cs001380@siu.buap.mx (G. Corro).

Table 1
Catalysts characterization data.

Reduced catalyst	Pt (wt%)	Pd (wt%)	Pt + Pd dispersion (%)
2%Pt/γ-Al$_2$O$_3$	2.1	–	40
1%Pd/γ-Al$_2$O$_3$	–	1.1	18
2%Pt–1%Pd/γ-Al$_2$O$_3$	2.0	1.1	27

In previous investigations on the oxidation of low concentration of methane in excess oxygen, we showed that pre-sulfating a Pt/γ-Al$_2$O$_3$ catalyst increased the oxidation activity and stability for this reaction relative to only reduced Pt/γ-Al$_2$O$_3$ catalyst. Pre-sulfation of the catalyst was performed by exposing the reduced catalyst for 4 h at 500 °C to a gas stream containing SO$_2$ and O$_2$ [21,22]. XPS data revealed the presence of metallic Pt(0) and the presence of Pt(IV) on this pre-sulfated Pt/γ-Al$_2$O$_3$ catalyst. It is well known that the oxidation of SO$_2$ to SO$_3$ is catalyzed by Pt at temperatures greater than 200 °C [23–25]. SO$_3$ can react with the Al$_2$O$_3$ support to form Al$_2$(SO$_4$)$_3$ and this reaction is further catalyzed by the presence of Pt [25]. Oxidation of SO$_2$ occurs via its dissociate adsorption on Pt [25–27]. SO$_2$ dissociate adsorption may be increased over Pt(0) related to Pt(IV) due to the higher electronic density in Pt(0), thus, to the higher interactions of Pt binding electrons with the anti-bonding orbital of the SO$_2$ molecule. These facts suggest that if a reduced Pt–Pd/γ-Al$_2$O$_3$ catalyst presents Pt(0) surface sites on which SO$_2$ would be preferentially adsorbed, then the probability of SO$_2$ adsorption on Pd surface sites may be lowered, since it is well known that the SO$_2$ intrinsic activity of Pd is lower than that of Pt [28]. Therefore, Pd surface sites activity for methane oxidation would be protected from deactivation due to sulfates formation. Therefore, the purpose of this study is to investigate the performance of a reduced Pt–Pd/γ-Al$_2$O$_3$ catalyst on methane oxidation in a SO$_2$ containing feed.

2. Experimental

2.1. Catalyst preparation

The support used was γ-Al$_2$O$_3$ Merck with a grain size of 0.063–0.200 mm (70–230 mesh ASTM), with a surface area of 165.52 m^2/g, and a pore volume of 0.60 cm^3/g. Pt, Pd and Pt–Pd catalysts supported on alumina were prepared by impregnation using aqueous solutions of Pt(NH$_3$)$_4$(NO$_3$)$_2$ and Pd(NH$_3$)$_4$(NO$_3$)$_2$ (Aldrich, min. 99% purity). After impregnation, the catalysts were dried at 120 °C overnight, and then calcined in flowing air for 6 h at 500 °C (called calcined catalysts). A sample of the calcined catalysts was reduced in pure hydrogen flow for 8 h at 500 °C (called reduced catalysts). A reference alumina support was prepared in the same way. A sample of the calcined or reduced catalysts was then sulfated. Sulfation was performed on the samples heating to 500 °C in flowing air (100 cm^3 min^{-1}), in order to eliminate any water traces in the support and prevent interactions between this water and SO$_2$ over the catalyst during the sulfation process. The feed was then changed at 500 °C for a nitrogen flow containing 50 ppm SO$_2$, 5% O$_2$ (100 cm^3 min^{-1}) for 4 h. The sample (called calcined-sulfated catalyst or reduced-sulfated catalyst) was then cooled to 25 °C.

The chemical microanalysis of the catalyst was determined by energy dispersive X-ray spectroscopy (EDS) (NORAN) performed in conjunction with a scanning electron microscope (JEOL, model JSM-6300). Catalysts metal contents are reported in Table 1.

2.2. Metal accessibility measurements

Platinum and palladium accessibility measurements on the reduced catalyst, were obtained by the irreversible H$_2$ chemisorption at room temperature in a static volumetric apparatus and using the stoichiometric (H/Pt–Pd)$_{surf}$ = 1. Isotherms were obtained in the 0–50 Torr (1 Torr = 1.33 mbar) range. Extrapolation of the linear part of the isotherm to zero pressure gave the monolayer coverage. This amount of H$_2$ chemisorbed in monolayer was then used to calculate the Pt + Pd dispersion.

2.3. XPS characterization

Photoelectron spectra were recorded over 2%Pt/γ-Al$_2$O$_3$, 1%Pd/γ-Al$_2$O$_3$, and 2%Pt-1%Pd/γ-Al$_2$O$_3$ using a VG Escalab 200R electron spectrometer equipped with a hemispherical analyzer, operating in a constant pass energy mode, and a monochromatic MgKα ($h\nu$ = 1253.6 eV, 1 eV = 1.603 × 10^{-19} J) X-ray source operated at 10 mA and 12 kV.

The energy regions of the photoelectrons of interest were scanned a number of times in order to get good signal-to-noise ratios, as due to the relative high surface area and the small particle size the photoelectron intensity was very low. The intensities of the peaks were estimated by determining the integral of each peak after subtracting an S-shaped background and fitting the experimental peak to Lorentzian/Gaussian lines (80%L/20%G). The binding energies (BE) were referenced to the Al2p peak, the BE of which was fixed at 74.5 eV. Using this reference, BE values of C1s peak coming from adventitious carbon appeared at 284.9 ± 0.2 eV.

2.4. Catalytic tests

The catalyst tests were performed in a continuous flow tubular quartz reactor (inner diameter 10 mm) placed in a programmable furnace. The catalyst temperature was controlled by a thermocouple mounted internally. Reactant gases were fed from independent mass flow controllers. Measurements over the samples were performed using a feed volume flow rate of 100 cm^3 min^{-1} consisting of 2000 ppmV CH$_4$, 10 vol.% of O$_2$, and balance He. The catalyst loading in the reactor was of 200 mg. The catalyst was not diluted with any inert component. The reactor out flow was analyzed using a Shimadzu gas chromatograph provided with a thermo-conductivity detector (TCD).

Before measuring the catalytic activity, the samples were pretreated for 1 h in the reactant stream at 600 °C. The samples were then cooled down (always in the reactant stream) to 25 °C and measurements used to determine the evolutions of CH$_4$ conversion as a function of temperature were made as the sample was heated in the range 25–600 °C at 10 °C min^{-1}. The samples were then cooled down again to 25 °C. The process comprising the methane oxidation from 25 to 600 °C is called a cycle. The catalyst was left at each temperature until the steady state was reached; usually 15 min was more than sufficient, but in the region of the 50% methane conversion, more than 1 h was required as a result of the exotherm generated. For the catalysts long time resistance test, ten similar cycles were performed over the same catalyst sample.

Temperature-programmed reaction profiles allowed us to determine the temperature at which methane conversion attains 50% (T_{50}) and 100% (T_{100}).

3. Results

3.1. Catalysts characterization

The reduced catalyst characterization data are summarized in Table 1. The H$_2$ chemisorption method cannot be applied to determine metal dispersions over calcined catalysts. H$_2$ isothermes are obtained over a clean surface after a reducing pretreatment in pure H$_2$. This pretreatment leads to reduced surface metallic species. Metal dispersion values for the catalysts after sulfation were not determined because the samples needed to be reduced again under

Table 2
Temperatures of 50% conversion (T_{50}) and of 100% conversion (T_{100}) for methane on CH_4–O_2 reaction over the catalysts studied.

Catalyst	T_{50} (°C)	T_{100} (°C)
Calcined samples		
2%Pt/γ-Al$_2$O$_3$	479	556
1%Pd/γ-Al$_2$O$_3$	373	450
2%Pt–1%Pd/γ-Al$_2$O$_3$	380	470
Calcined-sulfated samples		
2%Pt/γ-Al$_2$O$_3$	520	600
1%Pd/γ-Al$_2$O$_3$	420	500
2%Pt–1%Pd/γ-Al$_2$O$_3$	435	520
Reduced samples		
2%Pt/γ-Al$_2$O$_3$	462	556
1%Pd/γ-Al$_2$O$_3$	360	424
2%Pt–1%Pd/γ-Al$_2$O$_3$	373	440
Reduced-sulfated samples		
2%Pt/γ-Al$_2$O$_3$	420	500
1%Pd/γ-Al$_2$O$_3$	416	500
2%Pt–1%Pd/γ-Al$_2$O$_3$	387	475

a H$_2$ atmosphere at high temperature to reduce the metallic surface species. This reduction might have led to the reduction of sulfate to H$_2$S which poisons Pt sites.

3.2. Methane oxidation

In Table 2, the T_{50} and T_{100} for methane on CH_4–O_2 reaction over 2%Pt/γ-Al$_2$O$_3$, 1%Pd/γ-Al$_2$O$_3$ and 2%Pt–1%Pd/γ-Al$_2$O$_3$ catalysts are summarized. The γ-Al$_2$O$_3$ reference samples, prepared in the same way as the catalysts, were not active for methane oxidation at the temperature range studied in this work (25–600 °C).

3.2.1. 2%Pt/γ-Al$_2$O$_3$

In Fig. 1, we compare the evolution of CH_4 during CH_4–O_2 reaction as a function of temperature over 2%Pt/γ-Al$_2$O$_3$. In this figure and in Table 2, the following facts can be observed:

- A slight difference in T_{50} for methane was observed over calcined and reduced 2%Pt/γ-Al$_2$O$_3$ catalysts (479 °C and 462 °C, respectively).
- Sulfating the reduced 2%Pt/γ-Al$_2$O$_3$ resulted in an increase of the catalytic activity for CH_4–O_2 reaction, reflected by the decrease
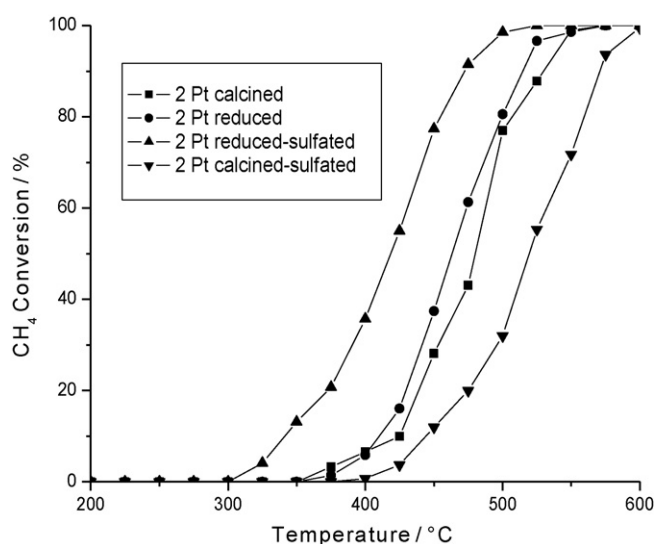

Fig. 1. Methane conversion as a function of temperature on the CH_4 + O_2 reaction over 2%Pt/γ-Al$_2$O$_3$ catalysts. Feed: 2000 ppmV CH_4, 10% O_2, balance N$_2$.
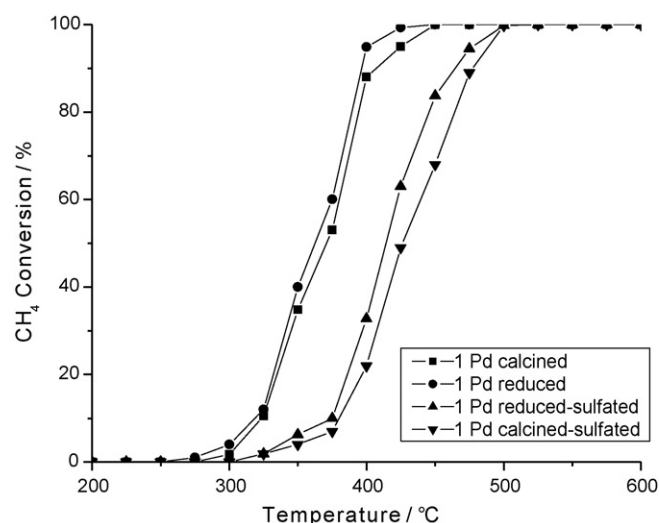
Fig. 2. Methane conversion as a function of temperature on the CH_4 + O_2 reaction over 1%Pd/γ-Al$_2$O$_3$ catalysts. Feed: 2000 ppmV CH_4, 10% O_2, balance N$_2$.

of the T_{50} for methane (462 °C for reduced catalyst and 420 °C for reduced-sulfated catalyst).

- When the calcined 2%Pt/γ-Al$_2$O$_3$ catalyst was sulfated, a strong decrease in activity for CH_4–O_2 reaction relative to only calcined catalyst was observed. The T_{50} for methane determined over calcined 2%Pt/γ-Al$_2$O$_3$ and calcined-sulfated 2%Pt/γ-Al$_2$O$_3$ were 479 °C and 520 °C, respectively.

3.2.2. 1%Pd/γ-Al$_2$O$_3$

Fig. 2 shows the evolution of CH_4 over 1%Pd/γ-Al$_2$O$_3$ catalysts as a function of the catalyst temperature. In this figure and in Table 2, it can be observed that:

- Similar activities for calcined 1%Pd/γ-Al$_2$O$_3$ and reduced 1%Pd/γ-Al$_2$O$_3$ were found for CH_4–O_2 reaction (as in the case of 2%Pt/γ-Al$_2$O$_3$). Similar values of T_{50} for methane were observed over calcined and reduced 1%Pd/γ-Al$_2$O$_3$ catalysts (373 °C or 360 °C, respectively).
- Sulfating the reduced 1%Pd/γ-Al$_2$O$_3$ or the calcined 1%Pd/γ-Al$_2$O$_3$ catalysts resulted in a deactivation of CH_4–O_2 reaction. Table 2 shows higher T_{50} for methane over sulfated samples related to only calcined or only reduced samples. It is evident that new inactive Pd sites were formed during sulfation.

3.2.3. 2%Pt–1%Pd/γ-Al$_2$O$_3$

The results from the CH_4 evolution as a function of the temperature measurements for CH_4–O_2 reaction over bimetallic 2%Pt–1%Pd/γ-Al$_2$O$_3$ catalyst are represented in Fig. 3. This figure and Table 2 show the following facts:

- Similar values of T_{50} for methane were observed over calcined 2%Pt–1%Pd/γ-Al$_2$O$_3$ and reduced 2%Pt–1%Pd/γ-Al$_2$O$_3$ catalyst (380 °C and 373 °C, respectively). In Table 2, it can be seen, that the activity of these calcined or reduced bimetallic catalysts is similar to the activity of monometallic calcined or reduced 1%Pd/γ-Al$_2$O$_3$ for CH_4–O_2 reaction.
- Sulfating the reduced 2%Pt–1%Pd/γ-Al$_2$O$_3$ catalyst resulted in a very small decrease of the catalytic activity for CH_4–O_2 reaction: T_{50} for methane values were observed at 373 °C for the reduced catalyst and at 387 °C for the reduced-sulfated catalyst.
- The effect of catalyst sulfation on CH_4–O_2 reaction over calcined 2%Pt–1%Pd/γ-Al$_2$O$_3$ resulted in a strong increase of the T_{50} for methane (380 °C for the calcined catalyst and 435 °C for calcined-

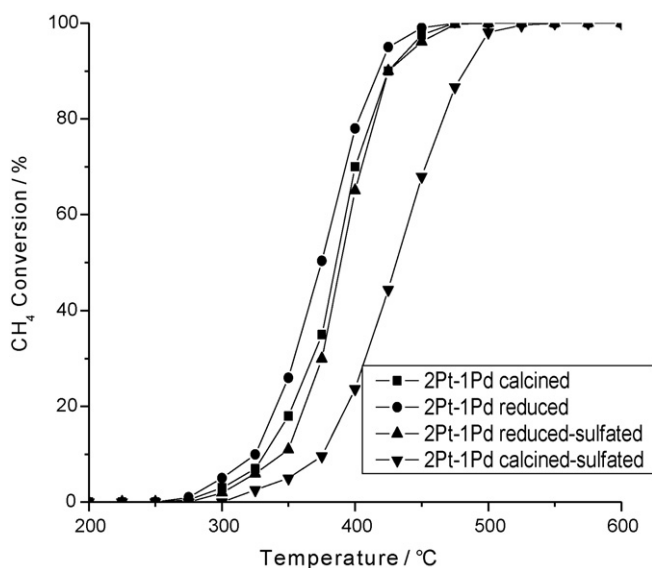**Fig. 3.** Methane conversion as a function of temperature on the $CH_4 + O_2$ reaction over 2%Pt–1%Pd/γ-Al_2O_3 catalysts. Feed: 2000 ppmV CH_4, 10% O_2, balance N_2.

sulfated catalyst). It is worth noting in Table 2, that the activity of calcined-sulfated bimetallic 2%Pt–1%Pd/γ-Al_2O_3 is very similar to the activity of calcined-sulfated monometallic 1%Pd/γ-Al_2O_3.

3.2.4. Effect of SO_2 in the CH_4–O_2 reaction feed

In order to simulate a long term exposure of the catalysts to sulfur containing compounds present in natural gas, the reduced 2%Pt–1%Pd/γ-Al_2O_3, and calcined 2%Pt–1%Pd/γ-Al_2O_3 were exposed to a reaction mixture containing SO_2. Ten temperature-programmed reaction cycles were performed over the catalysts.

After the 10 reaction cycles, the reduced 2%Pt–1%Pd/γ-Al_2O_3 was heated at 500 °C in a nitrogen flow containing 500 ppm SO_2 and 5% O_2 (100 cm^3 min^{-1}) for 50 h. After this catalyst ageing treatment, five additional CH_4–O_2 reaction cycles in the presence of 50 ppmV SO_2 were performed over the sample. Fig. 4 shows the effect of the presence of 50 ppmV SO_2 in the CH_4–O_2 reaction feed on the T_{50} for methane over these catalysts, and the effect of ageing treatment on reduced 2%Pt–1%Pd/γ-Al_2O_3.
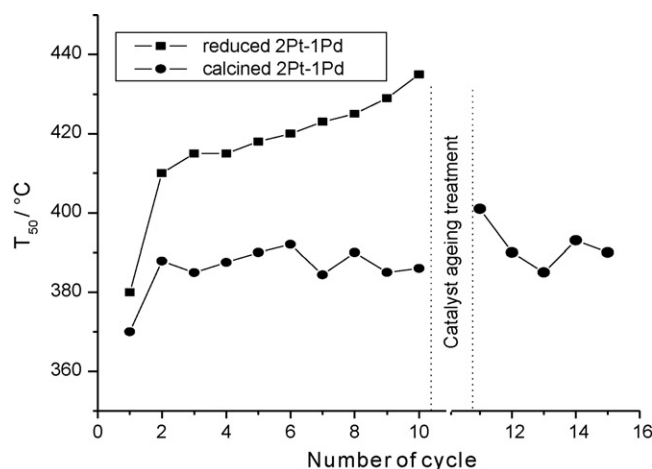

Fig. 4. Evolution of T_{50} for methane on the $CH_4 + O_2$ reaction, with the number of temperature-programmed reaction cycles over reduced 2%Pt–1%Pd/γ-Al_2O_3, and calcined 2%Pt–1%Pd/γ-Al_2O_3. Feed: 2000 ppmV CH_4, 10% O_2, 50 ppmV SO_2, balance N_2.

Table 3
Binding energies (eV) of core electrons of the catalysts studied.

Catalyst	$Pt4d_{5/2}$	$Pd3d_{5/2}$	$S2p$
2%Pt			
Calcined	317.2 (100)		–
Calcined-sulfated	317.1 (65), 318.4 (35)		169.1
Reduced	315.4 (58), 318.0 (42)		–
Reduced-sulfated	315.4 (52), 318.5 (42)		169.1
1%Pd			
Calcined		337.0	169.1
Calcined-sulfated		337.5	–
Reduced		336.3	169.1
Reduced-sulfated		337.5	–
2%Pt–1%Pd			
Calcined	317.1	337.0	169.1
Calcined-sulfated	317.1 (60), 318.3 (40)	337.5	–
Reduced	315.4 (50), 318.0 (50)	336.3	169.1
Reduced-sulfated	315.4 (52), 318.5 (48)	337.0	169.1

In parenthesis are peak percentages.

3.3. X-photoelectron spectroscopy

Binding energies of core electrons and atomic surface ratios determined by XPS are reported in Tables 3 and 4, respectively.

3.3.1. 2%Pt/γ-Al_2O_3

XPS spectra for $Pt4d_{5/2}$ on 2%Pt/γ-Al_2O_3 are displayed in Fig. 5. Binding energies of core electrons of calcined, reduced, and sulfated Pt catalysts are reported in Table 3. In this table, the following facts can be seen:

- For the calcined 2%Pt/γ-Al_2O_3 sample, the binding energy of the $Pt4d_{5/2}$, revealed only a binding energy component (317.2 eV) that shows that Pt is only present as Pt (II) [29–33].
- For the calcined-sulfated 2%Pt/γ-Al_2O_3 sample, the binding energy of the $Pt4d_{5/2}$, revealed a component at 317.2 eV and a higher binding energy component (318.4 eV) that can be associated to an increase in the highly oxidized Pt component with respect to the Pt (II) component.
- The binding energy $Pt4d_{5/2}$ for the reduced 2%Pt/γ-Al_2O_3 sample indicates that Pt is present as Pt (0) (315.4 eV). A second Pt component is observed at higher binding energies (318.0 eV) corresponding to an oxidized species of Pt. Now, it has been reported [30,31], for PtO_2 a binding energy component (318 eV) of the $Pt4d_{5/2}$ that can be assigned to Pt (IV).
- For the reduced-sulfated 2%Pt/γ-Al_2O_3 sample, the binding energies of the $Pt4d_{5/2}$, revealed that Pt is present as Pt (0) (315.4 eV). The higher binding energy component (318.5 eV) can be asso-

Table 4
Atomic surface ratios of the catalysts determined by XPS.

Catalyst	Pt/Al	Pd/Al	S/Pt	S/Pd
2%Pt				
Calcined	0.0038		–	
Calcined-sulfated	0.0020		0.82	
Reduced	0.0040		–	
Reduced-sulfated	0.0028		1.03	
1%Pd				
Calcined		0.0016		–
Calcined-sulfated		0.0012		0.23
Reduced		0.0018		–
Reduced-sulfated		0.0015		0.23
2%Pt–1%Pd				
Calcined	0.0036	0.0018		
Calcined-sulfated	0.0018	0.0012		
Reduced	0.0038	0.0019		
Reduced-sulfated	0.0025	0.0013		

Fig. 5. Pt $4d_{5/2}$ core level spectra 2%Pt/γ-Al$_2$O$_3$. (a) Calcined; (b) calcined-reduced; (c) reduced; (d) reduced-sulfated.

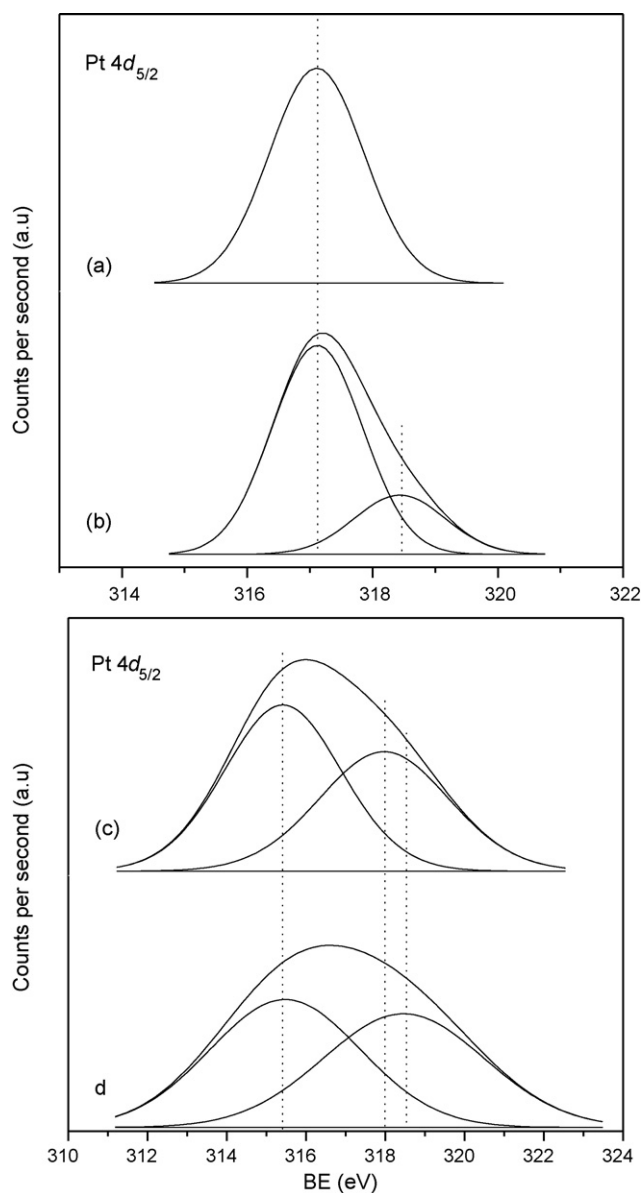**Fig. 6.** Pd3d core level XPS spectra of 1%Pd/γ-Al$_2$O$_3$. (a) Calcined; (b) calcined-reduced; (c) reduced; (d) reduced-sulfated.

ciated to an increase in the highly oxidized Pt component with respect to the Pt (0) component.

3.3.2. 1%Pd/γ-Al$_2$O$_3$

Fig. 6 shows the XPS spectra for Pd3d$_{5/2}$ on 1%Pd/γ-Al$_2$O$_3$ catalysts. In Table 3, it can be observed the binding energies of core electrons of calcined, reduced, and sulfated Pd catalysts.

- For the calcined sample, the binding energy Pd3d$_{5/2}$ showed a value of 337.0 eV. This value is too high for pure PdO, which presents a value of 336.7 eV [34,35] indicating the possibility of a mixture with Pd (IV) that presents a signal at 337.5 [36,37].
- For the calcined-sulfated sample, the binding energy of the Pd3d$_{5/2}$, revealed a signal at 337.5 eV with a S/Pd surface atomic ratio of 0.23 (shown in Table 4), which can be associated to the formation of a surface SO$_4^{2-}$. The effect of sulfating the calcined 1%Pd/γ-Al$_2$O$_3$ catalyst, resulted in an increase in the degree of Pd oxidation, as evidenced by the increase in the Pd3d$_{5/2}$ electron binding energy (from 337 eV to 337.5 eV), which can be asso-
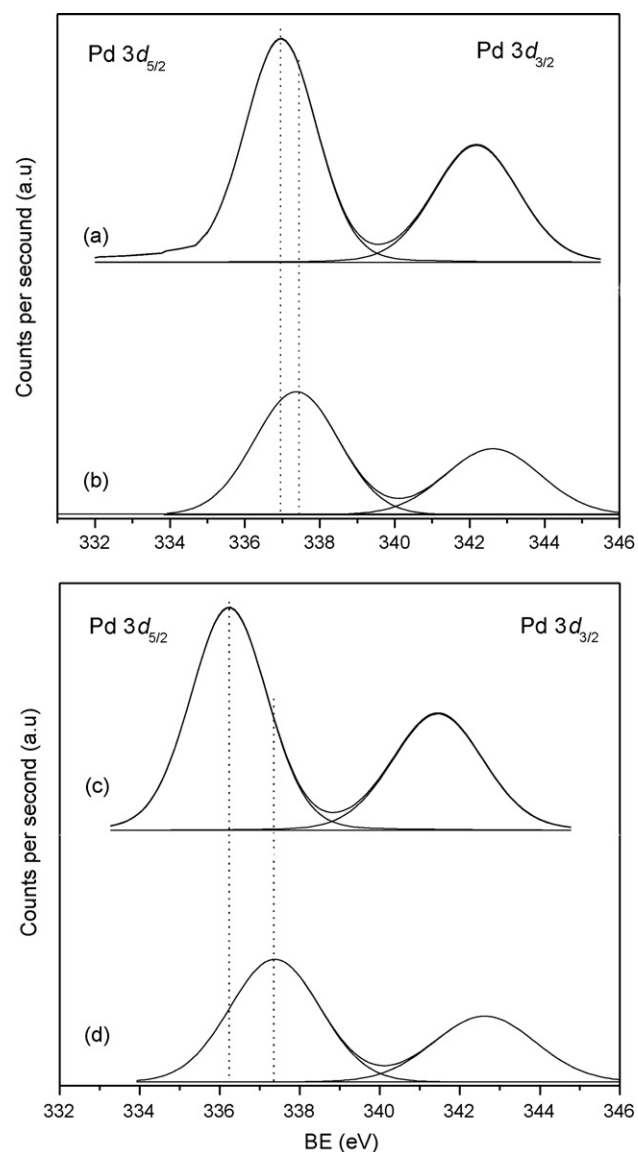
ciated to an oxidized Pd, probably in a SO$_x$–PdO species, as it was proposed earlier [3,39]. Now, Mowery and McCormick [45] report for a reference PdSO$_4$ a Pd 3d$_{5/2}$ binding energy at 338.5 eV. This binding energy is attributed to palladium sulfate, with a S/Pd atomic ratio of 1. However, for PdO exposed to SO$_2$ and CH$_4$ in air at 793 K, these authors report a Pd3d$_{5/2}$ binding energy at 336.9 eV with a S/Pd atomic ratio of 0.22. This value is higher than expected for Pd^{2+} in PdO but lower than the PdSO$_4$ reference. The same shift in the Pd binding energy is reported by Lampert et al. [3]. These authors report a Pd3d$_{5/2}$ binding energy at 337.5 eV with a S/Pd ratio of 0.23 after sulfation of a Pd/Al$_2$O$_3$ catalyst. These results suggest that the differences in the Pd 3d$_{5/2}$ binding energy values for the sulfated palladium samples depend on the S/Pd atomic ratio.
- The binding energy Pd3d$_{5/2}$ for the reduced 1%Pd/γ-Al$_2$O$_3$ sample indicates that Pd is present as Pd (II) (336.3 eV).
- The reduced-sulfated 1%Pd/γ-Al$_2$O$_3$ sample showed a signal at 337.5 eV, indicating as in the calcined-sulfated 1%Pd/γ-Al$_2$O$_3$ sample, the presence of SO$_x$–PdO species [3,39].
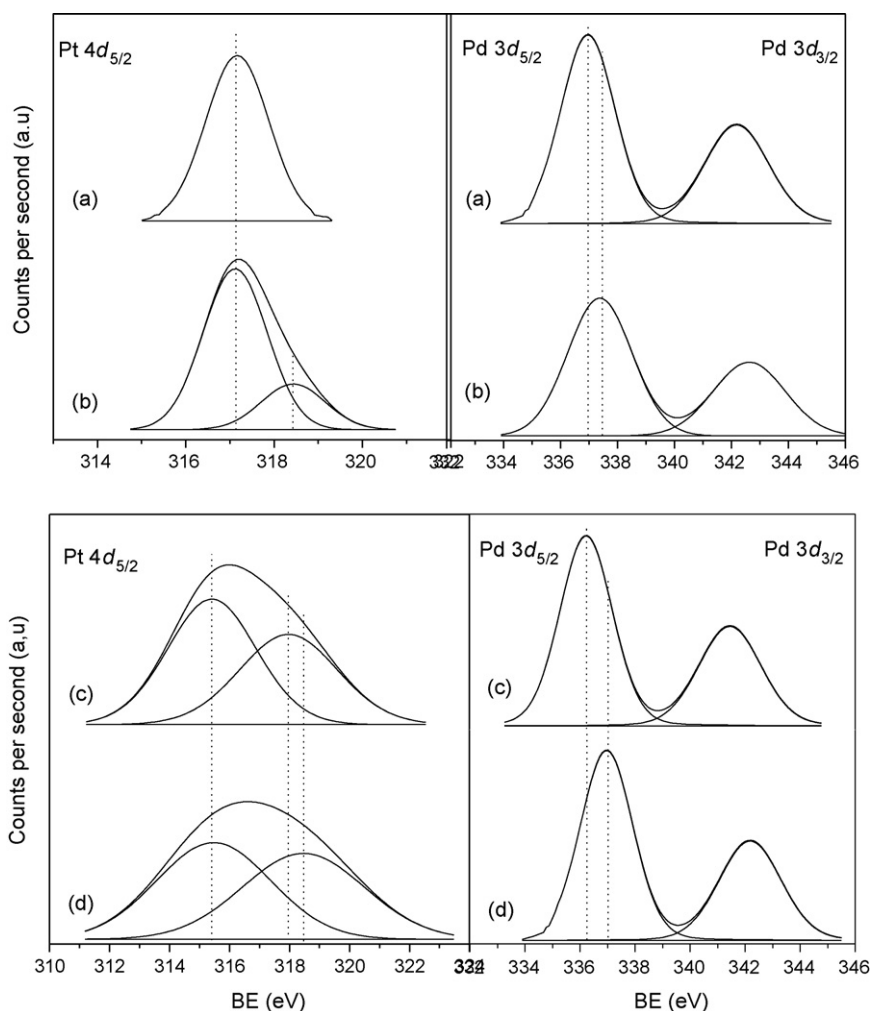
Fig. 7. Pt $4d_{5/2}$ core level and Pd 3d core level XPS spectra of 2%Pt–1%Pd/γ-Al$_2$O$_3$. (a) Calcined; (b) calcined-reduced; (c) reduced; (d) reduced-sulfated.

3.3.3. 2%Pt–1%Pd/γ-Al$_2$O$_3$

XPS spectra for Pt$4d_{5/2}$ and Pd$3d_{5/2}$ on 2%Pt–1%Pd/γ-Al$_2$O$_3$ are shown in Fig. 7. Binding energies of core electrons of the 2%Pt–1%Pd/γ-Al$_2$O$_3$ catalysts are reported in Table 3. These values indicate the following facts:

- The Pt$4d_{5/2}$ electron binding energies, observed in the bimetallic catalyst, independent of the pretreatment process, indicated no significant changes related to the Pt$4d_{5/2}$ electron binding energies in the monometallic 2%Pt/γ-Al$_2$O$_3$.
- No changes were observed for the binding energies of the Pd$3d_{5/2}$, determined over 1%Pd/γ-Al$_2$O$_3$ and over 2%Pt–1%Pd/γ-Al$_2$O$_3$ for calcined, calcined-sulfated, and reduced 2%Pt–1%Pd/γ-Al$_2$O$_3$.
- However, the Pd$3d_{5/2}$ electron binding energy observed in the reduced-sulfated 2%Pt–1%Pd/γ-Al$_2$O$_3$, revealed a signal at 337.0 eV which is lower than the Pd$3d_{5/2}$ electron binding energy observed in the reduced-sulfated monometallic 1%Pd/γ-Al$_2$O$_3$ (337.5 eV). This result suggests that the amount of SO$_x$–PdO species generated during sulfation is lower.

For the sulfated samples, the binding energy of the S$2p_{3/2}$ (168.9 eV) revealed that S is only present as S (VI) [29,38], thus only sulfate species are present in the catalyst.

4. Discussion

In this work, we investigated the possibility of obtaining a Pt–Pd/γ-Al$_2$O$_3$ catalyst which could lower palladium deactivation due to the presence of sulfur compounds in the reaction feed during methane oxidation.

4.1. 2%Pt/γ-Al$_2$O$_3$

In Fig. 1, it can be observed that the evolutions of CH$_4$ during CH$_4$–O$_2$ reaction as a function of temperature over calcined 2%Pt/γ-Al$_2$O$_3$ and reduced 2%Pt/γ-Al$_2$O$_3$ are very similar. However, XPS analysis revealed the presence of Pt (II) in the calcined 2%Pt/γ-Al$_2$O$_3$ sample and the presence of Pt (0) and Pt (IV) in the reduced 2%Pt/γ-Al$_2$O$_3$ sample. The different Pt electronic states present in each catalyst should result in different catalytic behavior for CH$_4$–O$_2$ reaction, but this is not the case. These results can be explained assuming that under oxygen excess conditions, all Pt surface sites on both catalysts are highly covered by adsorbed oxygen as proposed in previous investigations [39–41].

Sulfating the reduced 2%Pt/γ-Al$_2$O$_3$ resulted in an increase of the catalytic activity for CH$_4$–O$_2$ reaction. From these results, as reported in our previous investigations [21,22], it would appear that the activity of the catalytic sites for CH$_4$ oxidation are strongly

promoted by the presence of the new sites composed by Pt (IV) and the SO_4^{2-} generated during the sulfation process at the metal support interface over the catalyst. This assumption is supported by the XPS analysis (Table 3) that revealed a binding energy component of the $Pt4d_{5/2}$ at 318.5 eV which may correspond to the platinum species interacting with the SO_4^{2-} species at the metal support interface.

It is worth noting in Table 4 that sulfating the reduced $2\%Pt/\gamma$-Al_2O_3 resulted in a decrease in the Pt/Al atomic surface ratio (0.0040 for reduced $2\%Pt/\gamma$-Al_2O_3 and 0.0028 for reduced-sulfated $2\%Pt/\gamma$-Al_2O_3), thus in a decrease in the Pt surface area, thus in an increase in the metallic particle. The decreased Pt surface area should have resulted in a decrease in the Pt activity for the CH_4–O_2 reaction. However, this is not the case. These results can be explained assuming that the promoting effect of the new sites generated during sulfation of the reduced $2\%Pt/\gamma$-Al_2O_3 may largely compensate the loss in active surface area.

On the other hand, the binding energy component at 315.4 observed in reduced-sulfated $2\%Pt/\gamma$-Al_2O_3 revealed the presence of Pt (0). This result indicates that the high temperature reduction of the catalyst generated Pt species that remained at their metallic state despite the sulfation pretreatment.

Fig. 1 also shows that sulfating the calcined $2\%Pt/\gamma$-Al_2O_3 catalyst resulted in a strong decrease in activity for CH_4–O_2 reaction. This result can be explained considering that the size of the Pt particles increased upon exposure to a sulfur mixture at high temperature, as demonstrated previously by Chang et al. [42] and Lee et al. [43]. The increase in Pt particles may have resulted in a decrease in Pt surface atoms. This explanation is supported by the atomic surface ratios determined by XPS and shown in Table 4. In this table it can be seen that sulfating the calcined $2\%Pt/\gamma$-Al_2O_3 resulted in a decrease in the Pt/Al atomic surface ratio (0.0038 for calcined $2\%Pt/\gamma$-Al_2O_3 and 0.0020 for calcined-sulfated $2\%Pt/\gamma$-Al_2O_3).

Now, previous reports agree in that methane oxidation on Pt-based catalysts is promoted on larger Pt cristallites [44,39]. However, the loss of active sites by Pt sintering during sulfation process is higher than the promotion of methane oxidation on larger Pt cristallites. Thus, with increasing Pt particle size, there is a consequent loss in active surface area, resulting in a decrease in the catalytic activity for CH_4–O_2 reaction, as demonstrated by Garetto and Apesteguia [41].

4.2. $1\%Pd/\gamma$-Al_2O_3

XPS analysis revealed the presence of only Pd (II) over the reduced $1\%Pd/\gamma$-Al_2O_3 and a mixture of Pd (II) and Pd (IV) over the calcined $1\%Pd/\gamma$-Al_2O_3. However, Fig. 2 shows that calcined and reduced $1\%Pd/\gamma$-Al_2O_3 catalysts present similar activities for CH_4–O_2 reaction. The similarity of activities for both catalysts can be explained, assuming that during CH_4–O_2 reaction over the reduced $1\%Pd/\gamma$-Al_2O_3, Pd (IV) species may have been generated due to the presence of excess oxygen. Thus, during reaction, the active surface of reduced $1\%Pd/\gamma$-Al_2O_3 may be similar to the calcined $1\%Pd/\gamma$-Al_2O_3 active surface [3].

The deactivation of palladium catalysts due to sulfation is a very well known phenomenon [1,3,45–50] often referred to the formation of palladium sulfate species which are not active for the CH_4–O_2 reaction. Fig. 2 shows that sulfating the reduced $1\%Pd/\gamma$-Al_2O_3 or the calcined $1\%Pd/\gamma$-Al_2O_3 catalysts resulted in a strong deactivation for CH_4–O_2 reaction. It is evident that new inactive Pd sites were formed during sulfation. These sites may be probably SO_x–PdO species evidenced by XPS analysis which revealed a signal at 337.5 eV corresponding to these species on both sulfated catalysts.

4.3. $2\%Pt$–$1\%Pd/\gamma$-Al_2O_3

Table 2 and Figs. 2 and 3, show that the catalytic activity for CH_4–O_2 reaction of the calcined, calcined-sulfated, and reduced bimetallic $2\%Pt$–$1\%Pd/\gamma$-Al_2O_3 is similar to the activity of the calcined, calcined-sulfated, and reduced monometallic $1\%Pd/\gamma$-Al_2O_3, respectively. It would appear that the activity of the bimetallic catalyst is due only to the Pd active sites over the catalyst. Moreover, the results seem to show that Pt species do not interact with Pd species at the surface of the catalyst. XPS results support this observation: $Pt4d_{5/2}$ electron binding energies in the monometallic $2\%Pt/\gamma$-Al_2O_3 catalysts and $Pd3d_{5/2}$ electron binding energies in the monometallic $1\%Pd/\gamma$-Al_2O_3 catalysts are very similar to those determined for the bimetallic $2\%Pt$–$1\%Pd/\gamma$-Al_2O_3 catalysts. Moreover, Table 4 shows values for the atomic surface ratios for monometallic $2\%Pt/\gamma$-Al_2O_3 and monometallic $1\%Pd/\gamma$-Al_2O_3 very similar to those determined for the bimetallic $2\%Pt$–$1\%Pd/\gamma$-Al_2O_3.

A very interesting result is observed in Table 2 and in Fig. 3 which show that sulfating the reduced $2\%Pt$–$1\%Pd/\gamma$-Al_2O_3 catalyst resulted in only a very slight decrease of the catalytic activity for CH_4–O_2 reaction. It seems that the reduction of the catalyst at high temperature may have generated active Pt surface species able to prevent the deactivation of Pd surface species by sulfur deactivation. This assumption is supported by the XPS determinations on reduced-sulfated $2\%Pt$–$1\%Pd/\gamma$-Al_2O_3, shown in Table 3. In this table it can be seen the following facts:

- The $Pt4d_{5/2}$, electron binding energies observed in the reduced-sulfated $2\%Pt$–$1\%Pd/\gamma$-Al_2O_3 revealed a signal at 315.4 eV corresponding to metallic Pt(0) species. Now, it has been shown that the oxidation of SO_2 occurs via its dissociate adsorption on Pt [25–27], thus SO_2 dissociate adsorption may be increased over Pt(0) related to Pt(IV) due to the higher electronic density in Pt(0), thus, to the higher interactions of Pt binding electrons with the anti-bonding orbital of the SO_2 molecule. It is worth noting that metallic Pt(0) is present only in the reduced catalysts.
- The $Pd3d_{5/2}$ electron binding energy observed in the reduced-sulfated $2\%Pt$–$1\%Pd/\gamma$-Al_2O_3, at 337.0 eV which is lower than the $Pd3d_{5/2}$ electron binding energy observed in the reduced-sulfated monometallic $1\%Pd/\gamma$-Al_2O_3 (337.5 eV). This result suggests that the amount of SO_x–PdO species generated during sulfation is lower.

The results presented above suggest that the reduction of a bimetallic Pt–Pd/γ-Al_2O_3 catalyst in H_2 at high temperature may be necessary to generate Pt(0) sites which are active at adsorbing and oxidizing SO_2 present in the reaction flow in the CH_4–O_2 reaction. Based on the fact that the SO_2 intrinsic activity of Pd is lower than that of Pt [28], we assume that the presence of Pt(0) may lower the probability of SO_2 interactions with surface palladium species, thus may lower its deactivation at methane oxidation reaction.

Fig. 4 shows the effect of the presence of SO_2 on the evolution of T_{50} for methane as a function of the number of the temperature-programmed CH_4–O_2 reaction cycles. This figure shows that over calcined $2\%Pt$–$1\%Pd/\gamma$-Al_2O_3 catalyst, the presence of SO_2 in the reaction flow resulted in a strong increase of T_{50} for methane from the first CH_4–O_2 reaction cycle. This deactivation increased with the number of cycles and may be due to the formation of SO_x–PdO species generated by SO_2 interactions with palladium surface sites. However, over the reduced $2\%Pt$–$1\%Pd/\gamma$-Al_2O_3, the T_{50} for methane remains rather unaffected with the increase of CH_4–O_2 reaction cycles, despite the presence of SO_2 in the reaction flow. This results shows that the probability of SO_2 interaction with surface species on the reduced $2\%Pt$–$1\%Pd/\gamma$-Al_2O_3 may be higher on Pt(0) related to Pd species.

In order to study the long term effects of SO_2 deactivation in CH_4 oxidation, we treated the reduced 2%Pt–1%Pd/γ-Al_2O_3 (after 10 reaction cycles) in the ageing conditions described above. After this catalyst ageing treatment, five additional CH_4–O_2 reaction cycles in the presence of 50 ppmV SO_2 were performed over the sample. Fig. 4 shows a slight deactivation of the catalyst for methane oxidation after the ageing treatment. However, after two reaction cycles, the catalyst activity was completely recovered, e.g.: T_{50} for methane during the second reaction cycle after ageing treatment was 390 °C.

5. Conclusions

In this work, we investigated the possibility of obtaining a Pt–Pd/γ-Al_2O_3 catalyst which could lower palladium deactivation due to the presence of SO_2 in the reaction feed during methane oxidation.

Results showed that the reduced bimetallic 2%Pt–1%Pd/γ-Al_2O_3 catalysts presented a high resistance to deactivation by sulfur poisoning. The results are explained on basis of the XPS determinations revealing the presence of Pt metallic surface sites over the bimetallic catalyst. These metallic Pt sites may lower the probability of SO_2 interactions with surface palladium species, thus may lower its deactivation for methane oxidation reaction.

Acknowledgements

References

[1] P. Gélin, L. Urfels, M. Primet, E. Tene, Catal. Today 83 (2003) 45.
[2] D.L. Mowery, M.S. Graboski, T.R. Ohno, R.L. McCormick, Appl. Catal. B 21 (1999) 157.
[3] J.K. Lampert, M.S. Kazi, R.J. Farrauto, Appl. Catal. B 14 (1997) 211.
[4] W.C. Pfefferle, J. Energy 2 (1978) 142.
[5] M.F.M. Zwinkels, S.G. Järas, P.G. Menon, T.A. Griffin, Catal. Rev. Sci. Eng. 35 (1993) 319.
[6] D. Ciuparu, M.R. Lyubovsky, E. Altman, L.D. Pfefferle, A. Datye, Catal. Rev. 44 (2002) 593.
[7] K. Narui, H. Yata, K. Furuta, A. Nishida, Y. Kohtoku, T. Matsuzaki, Appl. Catal. A 179 (1999) 165.
[8] A. Ersson, H. Kusar, R. Carroni, T. Griffin, S. Jaras, Catal. Today 83 (2003) 265.
[9] K. Persson, A. Ersson, K. Jansson, N. Iverlund, S. Jaras, J. Catal. 231 (2005) 139.
[10] Y. Ozawa, Y. Tochihara, M. Nagai, S. Ami, Chem. Eng. Sci. 58 (2003) 671.
[11] D. Roth, P. Gélin, M. Primet, E. Tena, Appl. Catal. A 203 (2000) 37.
[12] T.V. Choudhary, S. Banerjee, V.R. Choudhary, Appl. Catal. A: Gen. 234 (2002) 1.
[13] F. Arosio, S. Colussi, G. Groppi, A. Trovarelli, Catal. Today 117 (2006) 569.
[14] A.M. Venezia, G. Di Carlo, G. Pantaleo, L.F. Liotta, G. Melaet, N. Kruse, Appl. Catal. B 88 (2009) 430.
[15] Y. Ozawa, Y. Tochihara, A. Watanabe, M. Nagai, S. Omi, Appl. Catal. A 259 (2004) 1.
[16] H. Yamamoto, H. Uchida, Catal. Today 45 (1998) 147.
[17] K. Nomura, K. Noro, Y. Nakamura, Y. Yazawa, H. Yoshida, A. Satsuma, T. Hattori, Catal. Lett. 53 (1998) 167.
[18] C.L. Pieck, C.R. Vera, E.M. Peirotti, J.C. Yori, Appl. Catal. A 226 (2002) 281.
[19] Y. Deng, T.G. Nevell, Catal. Today 47 (1999) 279.
[20] K. Persson, K. Jansson, S.G. Jarras, J. Catal. 245 (2007) 401.
[21] G. Corro, C. Cano, J.L. Garcia Fierro, J. Mol. Catal. A 281 (2008) 179.
[22] G. Corro, C. Cano, J.L. Garcia Fierro, Catal. Commun. 9 (2008) 2601.
[23] G.C. Bond, Catalysis by Metals, Academic Press, London, 1962.
[24] G.I. Godolets, Stud. Surf. Sci. Catal. 15 (1983) 365.
[25] D.D. Beck, M.H. Kruger, D.R. Monroe, SAE Paper no. 910844 (1991).
[26] U. Kohler, H.W. Wassmuth, Surf. Sci. 122 (1982) 491.
[27] R.C. Ku, P. Wynblatt, Appl. Surf. Sci. 8 (1981) 250.
[28] M. Horiuchi, Y. Ikeda, K. Sato, (1991), Exhaust Gas Purification Catalyst, U.S. Patent 5,000,929.
[29] D. Briggs, M.P. Seah (Eds.), Practical Surface Analysis by Auger and X-ray Photoelectron Spectroscopy, 2nd ed., Wiley, Chichester, UK, 1990.
[30] J. Escard, B. Pontvianne, M.T. Chenebaux, J. Cosyns, Bull. Soc. Chim. France 11 (1975) 2400.
[31] L. Guczi, A. Sarkany, Z. Koppany, Appl. Catal. 120 (1994) L1.
[32] E. Czaran, J. Finster, K.H. Schnabel, Z. Anorg. Allg. Chem. 443 (1978) 175.
[33] Z. Zsoldos, L. Guczi, J. Phys. Chem. 96 (1992) 23.
[34] D.H. Kim, S.I. Woo, J.M. Lee, O. Yang, Catal. Lett. 70 (2000) 35.
[35] K. Otto, L.P. Haak, J.E. de Vries, Appl. Catal. B 1 (1992) 1.
[36] Y. Bi, G. Lu, Appl. Catal. B 41 (2003) 279.
[37] A.L. Guimaraes, L.C. Dieguez, M. Schimai, J. Phys. Chem. B 107 (2003) 4311.
[38] C.D. Wagner, W.M. Riggs, L.E. Davis, J.F. Moulder (Eds.), Handbook of X-ray Photoelectron Spectroscopy, Perkin-Elmer Corporation, USA, 1990.
[39] Y.F.Y. Yao, Ind. Eng. Chem. Prod. Res. Dev. 5 (1980) 293.
[40] C.F. Cullis, D.E. Keene, D.L. Trimm, J. Catal. 19 (1970) 864.
[41] T.F. Garetto, C.R. Apesteguia, Catal. Today 62 (2000) 189.
[42] R.J. Chang, S.L. Chang, T.B. Lin, J. Catal. 169 (1997) 338.
[43] A.F. Lee, K. Wilson, R.M. Lambert, C.P. Hubbard, R.G. Hurley, R.W. McCabe, H.S. Gandhi, J. Catal. 184 (1999) 491.
[44] R.F. Hicks, H. Qi, M.L. Young, G.G. Lee, J. Catal. 146 (1994) 277.
[45] D.L. Mowery, M. McCormick, Appl. Catal. B: Environ. 34 (2001) 287.
[46] R. Burch, D.J. Crittle, B.W.L. Southward, J.A. Sullivan, Catal. Lett. 72 (2001) 153.
[47] J.M. Jones, A. Dupont, R. Brydson, D.J. Fullerton, Catal. Today 81 (2003) 589.
[48] V. Meeyoo, D.L. Trimm, N.W. Cant, Appl. Catal. B: Environ. 16 (1998) 105.
[49] S. Ordonez, P. Hurtado, H. Sastre, F.V. Diez, Appl. Catal. A 259 (2004) 41.
[50] Y. Deng, T.G. Novell, R.J. Ewen, C.L. Honeybourne, M.G. Jones, Appl. Catal. A 101 (1993) 51.